

## AN ALGORITHMIC APPROACH FOR PEAK LOAD EVALUATION OF STRUCTURAL ELEMENTS OBEYING A MENÉTREY-WILLAM TYPE YIELD CRITERION

AURORA ANGELA PISANO

ABSTRACT. A numerical procedure for the evaluation of the peak load of a general class of structures is presented. Namely the addressed structures obey to a three stress invariants constitutive criterion of Menétrey-Willam-type endowed with cap in compression. The formulation, developed in the Haigh-Westergaard coordinates, allows an easy treatment of the mechanical problem in a 3D context as well as an interesting geometrical interpretation in the principal stress space.

### 1. INTRODUCTION

The broadest area of success of plasticity theory with concrete structures is the treatment of situations in which the material acts primarily in compression. The usual procedure is nowadays to apply plasticity theory in the compression zone and treat the zones in which at least one principal stress is tensile by one of several version of fracture and/or damage mechanics also with the use of non local internal variables, see e.g. [1]. To guarantee a reliable design is essential to possess codes able to catch the behaviour of concrete structures even above the elastic limit; post elastic step-by-step analyses are the common tools available to this aim. However, the obtainable results, in the case of concrete elements, are strongly influenced by the dependence of strength, stiffness and ductility of this material on the load path. A valid alternative can be given by direct methods, i.e. the methods that are able to predict the load bearing capacity of a structure, or a structural element, in terms of peak load value, the one corresponding to the exhaustion of the strength capabilities, so avoiding any evolutive analysis.

A number of recent contributions are given in [11] and references therein. The numerical procedure for limit analysis, here adopted and known as *Linear Matching Method* (LMM), is the one originally proposed by Ponter and Carter [7] for Von Mises materials and recently generalized in Pisano and Fuschi [4, 5], Pisano et al [6], with reference to Tsai-Wu-type anisotropic, non associative composite plates. The method is here deeply reformulated in the Haigh-Westergaard coordinates with reference to a 3D-plasticity model for concrete with a pressure-sensitive yield surface with curved meridians in the Rendulic section,  $J_3$  dependence, cap in compression

---

2000 *Mathematics Subject Classification.* 65D25, 74S05, 74C05.

*Key words and phrases.* Numerical methods; finite element methods; rate-independent theory.  
©2012 Texas State University - San Marcos.

Submitted July 9, 2012. Published September 28, 2012.

and a non associated flow rule. The yield surface turns into the failure surface proposed by Menétrey and Willam [3], calibrated from elementary strength data and including the standard strength hypotheses of Huber-Mises, Drucker-Prager, Rankine, Mohr-Coulomb and Leon as special cases. The assumed yield surface is given in terms of three independent stress invariants and, in principal stress space it is convex and smooth. The LMM is applied to compute an upper bound to the peak load multiplier for simple concrete elements and one academic example is considered to estimate the gap between the computed upper bounds and the corresponding theoretical peak load values.

## 2. CONSTITUTIVE MODEL AND THEORETICAL BACKGROUND

The adopted three dimensional constitutive model for concrete is due to Menétrey and Willam [3]. It provides a three parameter failure surface having the following expression:

$$f(\xi, \rho, \theta) = \left[ \sqrt{1.5} \frac{\rho}{f'_c} \right]^2 + m \left[ \frac{\rho}{\sqrt{6} f'_c} r(\theta, e) + \frac{\xi}{\sqrt{3} f'_c} \right] - c = 0, \quad (2.1)$$

where

$$r(\theta, e) = \frac{4(1 - e^2) \cos^2 \theta + (2e - 1)^2}{2(1 - e^2) \cos \theta + (2e - 1) \left[ 4(1 - e^2) \cos^2 \theta + 5e^2 - 4e \right]^{1/2}}, \quad (2.2)$$

$$m := 3 \frac{f'_c{}^2 - f'_t{}^2}{f'_c f'_t} \frac{e}{e + 1}. \quad (2.3)$$

Equation (2.1) is expressed in terms of three stress invariants  $\xi, \rho$  and  $\theta$  known as the Haigh-Westergaard coordinates;  $m$  is the friction parameter of the material depending on the uniaxial compressive strength  $f'_c$ , on the uniaxial tensile strength  $f'_t$  as well as on the eccentricity parameter  $e$ . The eccentricity  $e$  defines the smoothness of the Menétrey-Willam surface and its value strongly influences the failure description either in biaxial tension or in compression. In (2.1),  $\xi$  is the hydrostatic stress invariant,  $\rho$  is the deviatoric stress invariant, and  $\theta$  is the deviatoric polar Lode angle; the Haigh-Westergaard (H-W) coordinates are given by

$$\xi = \frac{1}{\sqrt{3}} I_1, \quad I_1 = \sigma_{ii}, \quad (2.4)$$

$$\rho = \sqrt{2 J_2}, \quad J_2 = \frac{1}{2} s_{ij} s_{ij}, \quad (2.5)$$

$$\cos 3\theta = \frac{3\sqrt{3}}{2} \frac{J_3}{J_2^{3/2}}, \quad J_3 = \frac{1}{3} s_{ij} s_{jk} s_{ki}, \quad (2.6)$$

with  $s_{ij}$  denoting the deviatoric stress components; i.e.,  $s_{ij} = \sigma_{ij} - \frac{1}{3} \sigma_{kk} \delta_{ij}$  being  $\delta_{ij}$  the Kronecker symbol. It is worth to note that, for  $0 \leq \theta \leq \frac{\pi}{3}$ , the following relations, between principal stresses of  $\sigma_{ij}$  and H-W coordinates, hold:

$$\begin{Bmatrix} \sigma_1 \\ \sigma_2 \\ \sigma_3 \end{Bmatrix} = \frac{1}{\sqrt{3}} \begin{Bmatrix} \xi \\ \xi \\ \xi \end{Bmatrix} + \sqrt{\frac{2}{3}} \rho \begin{Bmatrix} \cos \theta \\ \cos(\theta - \frac{2\pi}{3}) \\ \cos(\theta + \frac{2\pi}{3}) \end{Bmatrix}. \quad (2.7)$$

The sector  $0 \leq \theta \leq \frac{\pi}{3}$  confining the values of the Lode angle  $\theta$  given by (2.6)<sub>1</sub> or, equivalently, by  $\cos \theta = (2\sigma_1 - \sigma_2 - \sigma_3)/2\sqrt{3}J_2$ , is consequence of a regular ordering of the eigenvalues of the stress tensor  $\sigma_{ij}$ ; i.e.,  $\sigma_1 \geq \sigma_2 \geq \sigma_3$ , as assumed in the

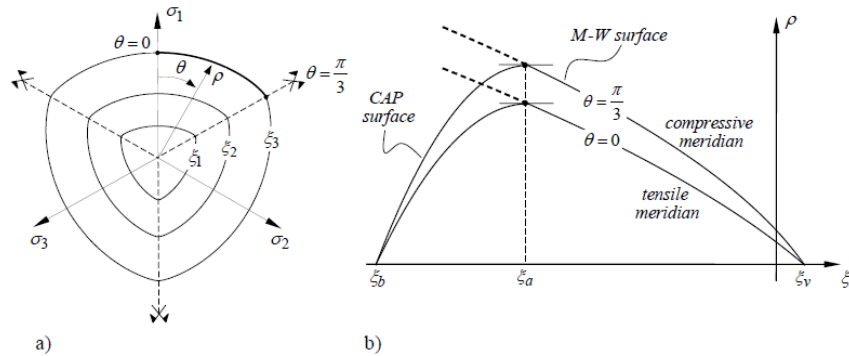


FIGURE 1. Triaxial failure surface of Menétrey-Willam with cap: (a) deviatoric sections at three generic values of hydrostatic pressure; (b) compressive and tensile meridians in the Rendulic plane

following. Remembering that the Lode angle  $\theta$  is the deviatoric projection of the angle between the radius vector of the current stress point in the principal stress space and the axis  $\sigma_1$ , the arbitrariness in the ordering of the eigenvalues of a tensor implies that six different points (i.e. six  $\theta$  values satisfying (2.6)<sub>1</sub>) correspond in the H-W representation to a given stress tensor. As a result, the M-W surface has to be symmetric with respect to the projections of the principal axes on the deviatoric plane. The surface represented by (2.1), defined for  $0 \leq \theta \leq \frac{\pi}{3}$ , so extends to all polar directions  $0 \leq \theta \leq 2\pi$  using the three-fold symmetry shown in Figure 1(a). The above condition is obviously met by the postulated isotropy of the material for which the labels 1,2,3 attached to the coordinate axes are arbitrary.

With the assumed ordering of the eigenvalues of the stress tensor there are two extreme cases:

$$\sigma_1 = \sigma_2 > \sigma_3; \quad \sigma_1 > \sigma_2 = \sigma_3; \quad (2.8)$$

corresponding to  $\theta = \frac{\pi}{3}$  and  $\theta = 0$ , respectively. The meridian at  $\theta = \frac{\pi}{3}$  is called *compressive meridian* (see also Figure 1(b)) in that (2.8)<sub>1</sub> represents a stress state corresponding to an hydrostatic stress state with a compressive stress superimposed in one direction. The meridian determined by  $\theta = 0$  (see again Figure 1(b)), represents an hydrostatic stress state with a tensile stress superimposed in one direction and is therefore called the *tensile meridian*. A realistic representation of concrete, viewed as a frictional material, requires to take into account the dilatancy, i.e. the volumetric expansion under compression. To this aim a *non associated flow rule* has to be *postulated*. Moreover, to capture the concrete behaviour near the hydrostatic axis, a *cap is adopted* to “close” the surface given by (2.1). This cap, in the H-W coordinates has the shape

$$\rho^{CAP}(\xi, \theta) = -\frac{\rho^{MW}(\xi_a, \theta)}{(\xi_a - \xi_b)^2} [\xi^2 - 2\xi_a(\xi - \xi_b) - \xi_b^2] \quad (2.9)$$

with  $\xi_b \leq \xi \leq \xi_a, \quad 0 \leq \theta \leq \frac{\pi}{3}$

where  $\rho^{MW}(\xi, \theta)$  is the explicit form of the parabolic meridian of the M-W surface that, looking at (2.1), can be given by the expression

$$\rho^{MW}(\xi, \theta) = \frac{1}{2a} \{-b(\theta) + [b^2(\theta) - 4ac(\xi)]^{1/2}\} \quad (2.10)$$

with  $\xi_a \leq \xi \leq \xi_v$ ,  $0 \leq \theta \leq \frac{\pi}{3}$

where:

$$a := \frac{1.5}{(f'_c)^2}, \quad b(\theta) := \frac{m}{\sqrt{6}f'_c} r(\theta, e), \quad c(\xi) := \frac{m}{\sqrt{3}f'_c} \xi - 1. \quad (2.11)$$

The three-fold symmetry of the M-W surface is maintained and the cap surface, given by (2.9), extends to all polar directions  $0 \leq \theta \leq 2\pi$  as sketched in Figure 1. The values  $\xi_a$  and  $\xi_b$  appearing in (2.9) locate the cap position that can be detected experimentally as given by Li and Crouch [2].

The Menétrey-Willam surface with a cap in compression is here assumed as yield criterion for the material, while the lack of associativity is overcome by means of the non-standard limit analysis approach [9].

### 3. THE KINEMATIC APPROACH OF LIMIT ANALYSIS AND THE LMM

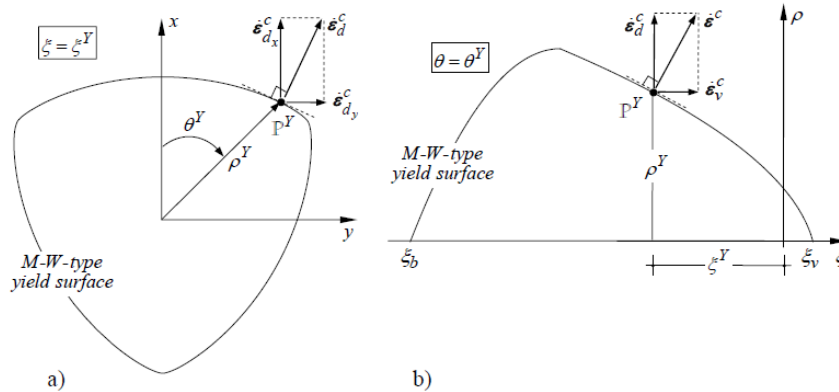


FIGURE 2. Stress point at yield  $\mathbb{P}^Y$ : (a) deviatoric section at  $\xi = \xi^Y$ ; (b) Rendulic section at  $\theta = \theta^Y$

To set the problem, let consider a body of volume  $V$  and external surface  $\partial V$  both referred to a Cartesian co-ordinate system  $(x_i, i = 1, 2, 3)$ . The body is, for simplicity, subjected only to surface loads  $P\bar{\mathbf{p}}(\mathbf{x})$ , where:  $P$  is a scalar load multiplier;  $\bar{\mathbf{p}}(\mathbf{x})$  denotes the reference load vector collecting all the surface force components,  $\bar{p}_i$ , acting on points of a portion of the body surface, namely  $\partial V_t$ . The remaining part of  $\partial V$ , namely  $\partial V_u = \partial V - \partial V_t$ , is assumed to suffer displacements  $\mathbf{u} = \mathbf{0}$ . Following the directions of non-standard limit analysis, reference can be made to a standard material "bounding from above" the real non-standard one and obeying to the same yield criterion. Rewriting the M-W-type yield criterion in the abridged form  $F(\xi, \rho, \theta) = 0$ , the volumetric and deviatoric strain rate components at collapse can be expressed in the form

$$\dot{\epsilon}_v^c = \lambda \frac{\partial F}{\partial \xi}; \quad \dot{\epsilon}_d^c = \lambda \frac{\partial F}{\partial \rho}; \quad (3.1)$$

with  $\dot{\lambda} \geq 0$  scalar multiplier. The kinematic approach of the limit analysis theory states that

$$P_{UB} \int_{\partial V_i} \bar{p}_i \dot{u}_i^c d(\partial V) = \int_V (\xi^Y \dot{\varepsilon}_v^c + \rho_x^Y \dot{\varepsilon}_{d_x}^c + \rho_y^Y \dot{\varepsilon}_{d_y}^c) dV. \quad (3.2)$$

In this equation,  $P_{UB}$  denotes the searched upper bound to the peak load multiplier;  $\dot{u}_i^c$  are the displacement rates at collapse of the points where surface loads,  $\bar{p}_i$ , act. Moreover,  $\dot{u}_i^c$  satisfy the condition  $\dot{u}_i^c = 0$  on  $\partial V_u$  and are compatible with the strain rates at collapse. Finally,  $\xi^Y$ ,  $\rho_x^Y$ ,  $\rho_y^Y$  are the stress components at yield associated to the volumetric and deviatoric strain rate components at collapse  $\dot{\varepsilon}_v^c$ ,  $\dot{\varepsilon}_{d_x}^c$ ,  $\dot{\varepsilon}_{d_y}^c$ , respectively. Referring to Figures 2(a)(b) an orthogonal cartesian system  $(x, y)$ , centered at  $\xi = \xi^Y$ , associated to the cylindrical coordinates  $(\xi, \rho, \theta)$  has been introduced for simplicity,  $(\cdot)_x$ ,  $(\cdot)_y$  denoting components of  $(\cdot)$  along  $x$  and  $y$  respectively. The set  $(\dot{\varepsilon}_v^c, \dot{\varepsilon}_{d_x}^c, \dot{\varepsilon}_{d_y}^c, \dot{u}_i^c)$ , if given at all stress point at yield (such as  $\mathbb{P}^Y$  in Figures 2(a)(b)), defines a collapse mechanism for the analyzed structure. The LMM in practice furnishes all the required quantities to compute a  $P_{UB}$ . The key idea is to build such quantities assuming the analysed structural element as made by a *linear viscous fictitious* material. This material is fictitious in the sense that it possesses *spatially varying moduli* and is also subjected to *imposed initial stresses*. A Finite Element (FE) analysis is performed on such fictitious structure so obtaining a fictitious solution. The fictitious moduli and initial stresses are then adjusted so that the computed fictitious stresses are brought on the yield surface at a fixed strain rate distribution. This allows one to define a collapse mechanism (compatible strain and displacement rates  $(\dot{\varepsilon}_v^c, \dot{\varepsilon}_{d_x}^c, \dot{\varepsilon}_{d_y}^c, \dot{u}_i^c)$ , plus related stresses at yield  $\xi^Y, \rho_x^Y, \rho_y^Y$ ) and, eventually, allows to evaluate a value of  $P_{UB}$ . Such procedure has to be carried on iteratively to satisfy the equilibrium conditions altered by the adjusting of the moduli and imposed stresses. A theoretical sufficient condition for convergence [8] assures the reliability of the final  $P_{UB}$ ; i.e., the one computed at last iteration.

**3.1. Geometrical interpretation of the LMM.** It is worth to remind the formal analogy existing between a linear viscous problem and a linear elastic problem on the basis of which the complementary dissipation rate function pertaining to the linear viscous problem plays the same role of the complementary energy potential function, say  $W$ , pertaining to the elastic problem. As a consequence, the fictitious linear solution (in terms of rate quantities) can be computed as fictitious elastic solution (in terms of finite quantities). In the H-W representation and for the chosen initial values (hereafter denoted by the apex  $(0)$ ) of material parameters and initial stresses,  $W$  can be given by the expression

$$W^{(0)}(\xi, \rho) = \frac{(\xi - \bar{\xi}^{(0)})^2}{6K^{(0)}} + \frac{(\rho - \bar{\rho}^{(0)})^2}{4G^{(0)}} = \bar{W}^{(0)}. \quad (3.3)$$

In equation,  $\bar{W}^{(0)}$  is a constant value,  $K^{(0)}$  and  $G^{(0)}$  are the initial elastic bulk and shear moduli respectively, while  $\bar{\xi}^{(0)}, \bar{\rho}_x^{(0)}, \bar{\rho}_y^{(0)}$  are the initial stresses. The volumetric and deviatoric strain rates of the linear problem can then be computed as:

$$\dot{\varepsilon}_v^\ell = \frac{\partial W^{(0)}}{\partial \xi}; \quad \dot{\varepsilon}_d^\ell = \frac{\partial W^{(0)}}{\partial \rho}. \quad (3.4)$$

The fictitious linear solution is also given in terms of compatible displacement rates of the points at which surface loads act, say  $\dot{u}_i^\ell$ , and in terms of stress values  $\xi^\ell, \rho_x^\ell, \rho_y^\ell$ , associated to the strain rate components  $\dot{\varepsilon}_v^\ell, \dot{\varepsilon}_{d_x}^\ell, \dot{\varepsilon}_{d_y}^\ell$ , respectively. The latter simply being the fictitious strain rates (3.4) referred to the orthogonal cartesian system  $(x, y, \xi)$  associated to the cylindrical H-W coordinates. Grounding on the above analogy, the fictitious linear analyses, involved by the LMM procedure, can be carried on at each iteration as fictitious elastic analyses performed by any commercial FE code, rendering the whole procedure easy.

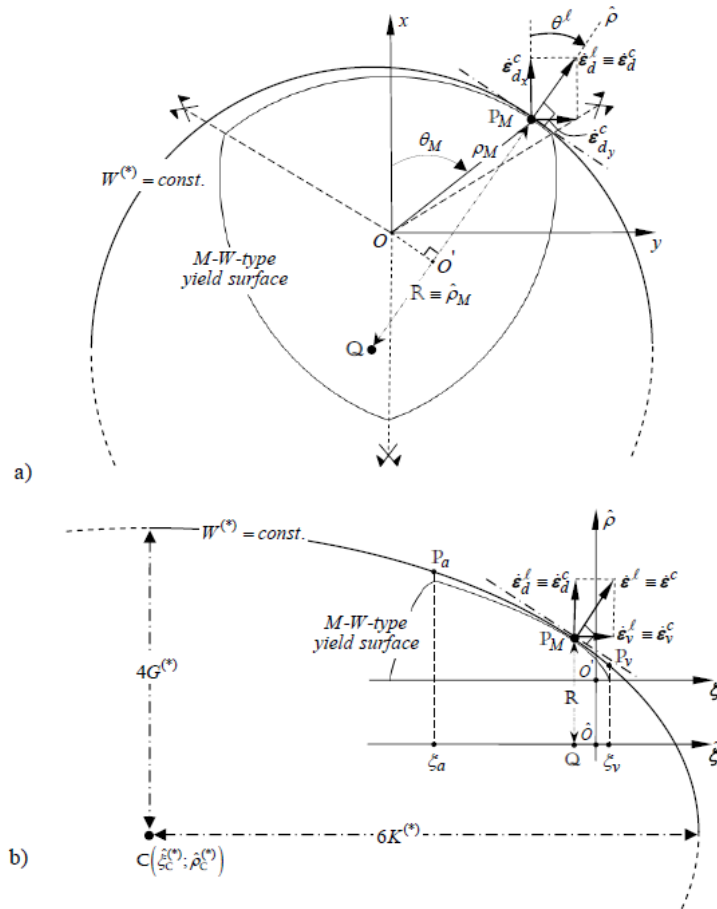


FIGURE 3. Construction of the prolate spheroid  $W^{(*)} = \text{const.}$  at matching: (a) deviatoric section, at  $\hat{\xi} = \xi = \xi_M$ , of the  $M$ - $W$ -type yield surface and of the spheroid  $W^{(*)} = \text{const.}$ ; (b) section on the plane belonging to the sheaf of axis  $\hat{\xi}$  and passing through  $P_M$

The above analogy leads also to an interesting geometrical interpretation of the LMM. First of all, as demonstrated in Ponter et al [8], a sufficient condition to assure convergence of the iterative procedure relies on a geometrical requirement; i.e., the

*complementary energy* equipotential *surface* of the fictitious material *at matching* (circumstance hereafter denoted by the apex  $(^{(*)})$ ) has indeed to touch the yield surface at the matching point  $\mathbb{P}_M$  but *must* otherwise *lie outside the yield surface* in stress space. In the specific case, with reference to (3.3), the complementary equipotential surface is a *prolate spheroid*; i.e., an *ellipsoid of revolution* obtained by rotating a generatrix ellipse about its major axis. As sketched in Figure 3(b), in the principal stress space, the semi-axes lengths of this spheroid at matching (say  $W^{(*)} = \text{const.}$ ) are related to the *unknown* values of the updated fictitious elastic moduli  $K^{(*)}$  and  $G^{(*)}$ . Its origin,  $\mathbb{C}$ , is located by the *unknown* values of the updated initial hydrostatic pressure and deviatoric stresses  $\bar{\xi}^{(*)}, \bar{\rho}_x^{(*)}, \bar{\rho}_y^{(*)}$ . In order to satisfy either the matching or the sufficient condition for convergence the elastic moduli and the initial stresses must be updated, at each iteration, according to the following requisites to be met by the complementary energy surface  $W^{(*)} = \text{const.}$ :

- (i) it must contain the matching point  $\mathbb{P}_M$ ;
- (i) it has to be tangent in  $\mathbb{P}_M$  to the M-W-type yield surface admitting at  $\mathbb{P}_M$  outward normal equal to  $\hat{\epsilon}^\ell \equiv \hat{\epsilon}^c$ ;
- (ii) it has otherwise lie outside the yield surface. The latter requisite can be easily accomplished by imposing that the ellipse passes through points (outer to the yield surface but “below” the tangent through  $\mathbb{P}_M$ ) like  $\mathbb{P}_a$  and  $\mathbb{P}_v$  at  $\hat{\xi} = \xi_a$  and  $\hat{\xi} = \xi_v$ , respectively, shown in Figure 3(b) for a  $\mathbb{P}_M$  on the M-W surface. Analogously it can be done for a  $\mathbb{P}_M$  on the cap.

All the above conditions yield to a non linear system of five equations to be solved at each Gauss point of each finite element in the mesh. In the next section the whole procedure is presented in a flow-chart style.

### 3.2. Flow-chart of the iterative scheme of LMM.

- *Initialization*

Assign to all FEs an initial set of fictitious elastic parameters, say  $E^{(0)}, G^{(0)}, \nu^{(0)}$ , and initial stresses  $\bar{\xi}^{(0)}, \bar{\rho}_x^{(0)}, \bar{\rho}_y^{(0)}$ . Set also:  $k = 1, P_{UB}^{(k-1)} = P_{UB}^{(0)} = 1$  (for  $k = 1, P_{UB}^{(0)}$  can be any arbitrary value) and compute the bulk modulus  $K^{(0)} = E^{(0)} / 3(1 - 2\nu^{(0)})$ .

- *Start iterations*

**Step 1:** perform a fictitious elastic analysis with elastic parameters  $E^{(k-1)}, G^{(k-1)}, \nu^{(k-1)}$ ; initial stresses  $\bar{\xi}^{(k-1)}, \bar{\rho}_x^{(k-1)}, \bar{\rho}_y^{(k-1)}$ ; loads  $P_{UB}^{(k-1)} \bar{p}_i$  (at the first iteration use the initialization quantities). Compute a fictitious linear solution (at Gauss point level), namely:  $\dot{\epsilon}_v^{\ell(k-1)}, \dot{\epsilon}_{d_x}^{\ell(k-1)}, \dot{\epsilon}_{d_y}^{\ell(k-1)}, \dot{u}_i^{\ell(k-1)}$  together with the stress values  $\xi^{\ell(k-1)}, \rho_x^{\ell(k-1)}, \rho_y^{\ell(k-1)}$ .

**Step 2:** compute the constant value of the complementary potential energy for later use:

$$\bar{W}^{(k-1)} = \frac{1}{2} \xi^{\ell(k-1)} \dot{\epsilon}_v^{\ell(k-1)} + \rho_x^{\ell(k-1)} \dot{\epsilon}_{d_x}^{\ell(k-1)} + \rho_y^{\ell(k-1)} \dot{\epsilon}_{d_y}^{\ell(k-1)}$$

**Step 3:** impose the matching conditions to update the fictitious quantities:  $\hat{\xi}_C^{(k)}, \hat{\rho}_C^{(k)}, G^{(k)}, K^{(k)}, \Omega^{(k)}$  to be used, if necessary, at next iteration (refer also to Figures 3(a)(b))

$$\frac{\hat{\xi}_M^{(k-1)} - \hat{\xi}_C^{(k)}}{3K^{(k)}} = \dot{\epsilon}_v^{\ell(k-1)},$$

$$\frac{\hat{\rho}_M^{(k-1)} - \hat{\rho}_C^{(k)}}{2G^{(k)}} = \dot{\varepsilon}_d^{\ell^{(k-1)}},$$

$$\frac{[\hat{\xi}_{\mathbb{P}_i}^{(k-1)} - \hat{\xi}_C^{(k)}]^2}{6K^{(k)}\Omega^{(k)}\bar{W}^{(k-1)}} + \frac{[\hat{\rho}_{\mathbb{P}_i}^{(k-1)} - \hat{\rho}_C^{(k)}]^2}{4G^{(k)}\Omega^{(k)}\bar{W}^{(k-1)}} = 1 \quad \text{with } i = a, v, M.$$

**Step 4:** evaluate the upper bound multiplier

$$P_{UB}^{(k)} = \frac{\int_{\partial V_i} \bar{p}_i \dot{u}_i^{c(k-1)} d(\partial V)}{\int_V \left( \xi^{Y(k-1)} \dot{\varepsilon}_v^{c(k-1)} + \rho_x^{Y(k-1)} \dot{\varepsilon}_{d_x}^{c(k-1)} + \rho_y^{Y(k-1)} \dot{\varepsilon}_{d_y}^{c(k-1)} \right)}$$

**Step 5:** check for convergence

$$|P_{UB}^{(k)} - P_{UB}^{(k-1)}| \leq \text{TOL} \quad \begin{cases} \text{YES} & \Rightarrow \text{EXIT} \\ \text{NOT} & \Rightarrow \text{set } k = k - 1 \text{ and GOTO step 1} \end{cases}$$

• *End iterations*

#### 4. NUMERICAL APPLICATION AND CONCLUDING REMARKS

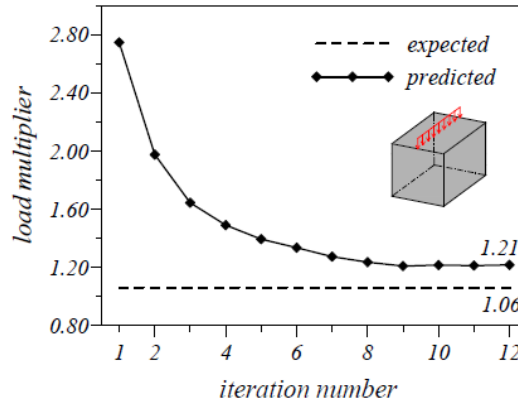


FIGURE 4. Values of the upper bound  $P_{UB}$  to the peak load multiplier versus iteration numbers for a cubic concrete sample subjected to a central line load

The reliability of the discussed approach is verified by a simple numerical application of engineering interest concerning a cubic concrete sample of side  $d = 150$  mm, with:  $E = 0.588$  GPa;  $\nu = 0.2$ . Moreover, referring to Eqs.(2.1-3), the following material data have been assumed:  $f'_c = 30$  MPa,  $f'_t = 3$  MPa and  $e = 0.539$ . The sample is subjected to a central line reference load of global value equal to 100 kN. The expected peak load is given by the formula  $P_U = \pi d^2 f_{st} / 2 \bar{p}$ , after [10], with  $f_{st} = f'_t / 0.9885$  so that, for the given data, the expected peak load multiplier is  $P_U = 1.06$ . All the elastic analyses have been carried out using the FE code ADINA, with meshes of 3D-Solid elements, while a Fortran main program has been developed to drive the iterative procedure and the matching at each Gauss point. Figure 4 shows the numerical evaluated upper bound to the peak load multiplier,



$P_{UB}$ , versus the iteration number. A monotonic and rapid convergence of the iterative procedure is exhibited and the numerical  $P_{UB}$  value appears to be quite close to the expected one. Even if the considered example is simple, the obtained results seems to be quite encouraging, comparison with experimental findings on concrete prototypes of engineering interest exhibiting a greater complexity are the object of an ongoing research.

## REFERENCES

- [1] M. Jirásek, Z.P. Bažant; *Inelastic Analysis of Structures*, John Wiley & Sons, LTD, West Sussex, England, (2002).
- [2] T. Li, R. Crouch; *A  $C_2$  plasticity model for structural concrete*. Computers and Structures **88** (2010), 1322-1332.
- [3] P. Menétrey, K.J. Willam; *A triaxial failure criterion for concrete and its generalization*. ACI Structural Journal **92**, 311-318.
- [4] A. A. Pisano, P. Fuschi; *A numerical approach for limit analysis of orthotropic composite laminates*. Int. J. Numerical Methods Eng **70** (2007), 71-93.
- [5] A. A. Pisano, P. Fuschi; *Mechanically fastened joints in composite laminates: Evaluation of load bearing capacity*. Composites: Part B **42** (2011), 949-961.
- [6] A. A. Pisano, P. Fuschi, D. De Domenico; *A layered limit analysis of pinned-joints composite laminates: Numerical versus experimental findings*. Composites: Part B **43** (2012), 940-952.
- [7] A. R. S. Ponter, K. F. Carter; *Limit state solutions, based upon linear elastic solutions with spatially varying elastic modulus*. Comput Methods Appl Mech Eng **140** (1997), 237-258.
- [8] A. R. S. Ponter, P. Fuschi, M. Engelhardt; *Limit analysis for a general class of yield conditions*. Eur. J. Mechanics/A Solids **19** (2000), 401-421.
- [9] D. Radenkovic; *Théorèmes limites pour un matériau de Coulomb à dilatation non standardisée*. CR Acad Sci Paris **252** (1961), 4103-4104.
- [10] C. Rocco, G.V. Guinea, J. Planas, M. Elices; *Size effect and boundary conditions in the Brazilian test: theoretical analysis*. Materials and Structures **32** (1999), 437-444.
- [11] D. Weichert and A. R. S. Ponter, Eds.; *Limit States of Materials and Structures - Direct Methods*, Springer Verlag, Wien (2009).

AURORA A. PISANO

DEPARTMENT PAU, UNIVERSITY MEDITERRANEA OF REGGIO CALABRIA, FEO DI VITO, 89100 REGGIO CALABRIA, ITALY

E-mail address: [aurora.pisano@unirc.it](mailto:aurora.pisano@unirc.it)